J Mater Sci: Mater Electron (2015) 26:7873–7881
DOI 10.1007/s10854-015-3438-9

Thickness effects on optical and photoelectric properties of PbSeTeO quaternary thin films prepared by magnetron sputtering

Xigui Sun[1] · **Kewei Gao**[1] · **Xiaolu Pang**[1] · **Huisheng Yang**[1] · **Alex A. Volinsky**[2]

Received: 20 May 2015 / Accepted: 29 June 2015 / Published online: 15 July 2015

Abstract PbSeTeO quaternary thin films with different thickness were grown on Si(100) substrates by magnetron sputtering. The as-prepared thin films show face centered cubic crystal structure and the main diffraction peak varied from PbSe(220) to PbSe(200) with the film thickness due to the transition between the surface energy and the strain energy contributions to the growth mechanism. A red shift of the absorption edge from 2200 cm^{-1} (4.55 μm) to 1400 cm^{-1} (7.14 μm) with the film thickness was obtained, indicating that increasing the thickness is an effective method to expand the absorption range of the sputtered PbSeTeO quaternary thin films. The photoelectric sensitivity increased almost linearly with the film thickness. This is attributed to the decrease of the density of states (DOS) near the top of the valence band, the increase of DOS near the conduction band bottom and the narrowing of the optical band gap calculated by the generalized gradient approximation with the Perdew–Burke–Ernzerhof exchange correlation functional formalism.

1 Introduction

Lead chalcogenides have been widely used as infrared detectors [1], laser diodes [2], thermoelectric devices [3], solar cells [4], etc. The absorption range of these materials covers 3–30 μm, since the band gaps can be varied from 0 to 0.5 eV by adjusting the film composition and operating temperature [5]. Among these lead chalcogenides, lead selenide (PbSe) thin films have attracted wide attention due to their unique properties. PbSe is a narrow and direct band gap IV–VI semiconductor, which has ten valence electrons instead of eight electrons for common III–V (ex. GaAs) and II–VI (ex. ZnS) compounds [6]. Besides, PbSe has high carrier mobility and large dielectric constant, leading to the PbSe devices maintaining superior performance within a wide working temperature range [7].

Generally, optical and photoelectric properties of the PbSe thin films can be improved by doped with other elements, such as Te [8], S [9], Sn [10], Cd [11], Sr [12], etc., since the band structure, especially the band gap and the density of states (DOS) of PbSe, can be modified by these doping elements. Te element has attracted great attention due to the superior photoelectric and thermoelectric properties of the PbSeTe materials. Kumar et al. [13] characterized the optical and electrical properties of the $PbSe_{1-x}Te_x$ thin films, and found that the band gap and conductivity varied dramatically with the composition of the thin films. Naeemullah et al. [14] studied the structural and optoelectronic properties of $PbSe_xTe_{1-x}$ via first principles calculations, and suggested that the maximum optical conductivity of these materials in the 2–4 eV range makes them usable as solar cells and various detectors. On the other hand, the maximum reflection of these materials is above 50 %, allowing high frequency radiation shielding application. Generally, further sensitizing treatment, also known as oxidizing treatment, is necessary to improve the photoelectric properties of the PbSe thin films [15]. Gautier et al. [16] found that the oxygen-induced sensitization could alter the microstructure, phase composition, and consequently optical and photoelectric properties of the polycrystalline PbSe thin films. Besides, Jung et al. [17]

✉ Xiaolu Pang
pangxl@mater.ustb.edu.cn

[1] Department of Materials Physics and Chemistry, University of Science and Technology Beijing, Beijing 100083, China

[2] Department of Mechanical Engineering, University of South Florida, Tampa, FL 33620, USA

demonstrated that the oxidized surface of the PbSe nanowires prepared by the radio frequency magnetron sputtering significantly affects their optical properties and creates strong confined states. However, few of the current literature reports dealt with the sensitizing treatment during the deposition process. This can create homogeneous distribution of oxygen atoms in the thin films, requiring further studies.

Until now, the lead chalcogenides thin films have been successfully prepared by using chemical bath deposition [18], electrochemical deposition [19], thermal evaporation [20] and molecular beam epitaxy [21], etc. Magnetron sputtering has been widely used to prepare semiconductor thin films, outperforming other deposition techniques [22]. Jdanov et al. [23] have used magnetron sputtering to deposit PbTe thin films on Si(111) substrates, and the as-prepared thin films show high crystallinity. However, these sputtered thin films were quite thin (80–300 nm) due to the high stresses developed in the films, inhibiting thicker films deposition. Hence, it is essential to decrease the film stresses and increase the film thickness to expand the application range. On the other hand, the photoelectric and optical properties of the lead chalcogenides thin films vary with the film thickness due to the evolution of the microstructure and lattice constant [24, 25]. However, the mechanism is unclear, and it is necessary to explain these results based on the atomic scale.

In this paper, three PbSeTeO quaternary thin films with different thickness were grown on Si(100) by magnetron sputtering, studying the thickness effects on the crystal structure, optical properties and photoelectric sensitivity by field emission scanning electron microscopy (FE-SEM), X-ray diffraction (XRD), X-ray photoelectron spectroscopy (XPS) and Fourier transform infrared spectroscopy (FT-IR). Interestingly enough, the photoelectric sensitivity of the sputtered PbSeTeO quaternary thin films increased almost linearly with the film thickness due to the band gap and DOS variations, confirmed by theoretical calculations based on the generalized gradient approximation (GGA) with the Perdew–Burke–Ernzerhof (PBE) exchange correlation functional formalism.

2 Experimental

2.1 Deposition

Three PbSeTeO quaternary thin films with different thickness were grown on the Si(100) substrates under 5×10^{-3} Pa base pressure by the PM500-S magnetron sputtering system equipped with the MF-5K medium frequency power source. The PbSeTe ternary alloy targets used in this research were hot pressed PbSeTe powders (n_{Pb}:n_{Se}:n_{Te} = 47.5:47.5:5) with 99.99 % purity. During the deposition process, high purity Ar gas (99.99 %) used as the sputtering ions were introduced into the sputtering chamber with a constant flux of 30 standard cubic centimeters per second (sccm) controlled by a mass flow controller. Since oxygen atoms can act as the "sensitizer", which improves the photoelectric sensitivity of the PbSe thin films [25], oxygen was introduced into the sputtering chamber with a constant flux of 1 sccm during the sputtering process. The deposition time was set to 120, 180 and 240 min, corresponding to the film thickness of about 420, 650 and 860 nm, respectively.

2.2 Characterization

The surface and cross-section morphology of the sputtered PbSeTeO quaternary thin films were characterized by the field emission scanning electron microscopy (FE-SEM, Zeiss Auriga) with 15 kV operating voltage. The crystal structure was studied using the rotating anode diffractometer (Dmax-RB 12 kW, Rigaku) with the Cu radiation source ($\lambda = 1.5406$ Å) in the 2θ angle ranged from 10° to 65°.

The XPS measurements were conducted on the thin films surface by using the AXIS ULTRA^{DLD} (SHIMADZU) X-ray photoelectron spectrometer equipped with the Al Kα source, $h\nu = 1486.6$ eV. Further XPS measurements were performed after the film surface was etched for 60 s by Ar^{+} with 3000 eV etching energy to study the oxidation layer and the difference of the chemical states in the film.

Photoelectric properties of the sputtered PbSeTeO quaternary thin films were characterized by the two-probe method in a dark chamber equipped with a 275 W infrared light source and a digital ohmmeter. The charge carriers concentration and mobility of the PbSeTeO thin films were measured by the Hall effect measurements performed using the physical properties measurement system (PPMS) with 7000 Gs magnetic field intensity and 0.7 μA current at room temperature.

Optical properties of the thin films were studied by the infrared absorption spectra recorded on the Nicolet Nexus 470 Fourier transform infrared spectrometer (FT-IR) ranging from 4000 to 400 cm^{-1} at room temperature.

3 Results and discussion

3.1 Microstructure

It is essential to obtain thin films with high surface quality, since the performance of the thin film devices, especially their lifetime, is seriously affected by the surface roughness and cracks [26]. As seen in Fig. 1a, the surface of sputtered PbSeTeO quaternary thin films is quite smooth and crack-free, indicating the applicability of magnetron sputtering. According to the cross-section images shown in Fig. 1b, the film thickness, δ, is about 420, 650 and 860 nm for the PbSeTeO thin films deposit 120, 180 and 240 min, respectively, as listed in Table 1. The film thickness increases almost linearly with the deposition time, as shown in Fig. 1c, and the deposition rate of the sputtered PbSeTeO quaternary thin films is about 3.6 nm/min.

Generally, the band structure of the semiconductor materials is severely affected by the crystal structure, which consequently affects their photoelectric properties [27].

Figure 2 shows the XRD patterns of the sputtered PbSeTeO quaternary thin films prepared with different deposition time. Compared with the JCPDS PDF cards, all diffraction peaks are attributed exclusively to the PbSe phase due to low content or crystallinity of other phases. Diffraction peaks at about 25°, 29°, 41°, 49° and 60° are attributed to PbSe(111), PbSe(200), PbSe(220), PbSe(311) and PbSe(400), respectively, indicating the face centered cubic crystal structure of the sputtered PbSeTeO quaternary thin films.

It is interesting to note that the main growth direction changes from [220] to [200] orientation when the film thickness exceeds 650 nm, which may be attributed to the transition of the controlling factor of the film growth. Generally, the growth mechanism of the sputtered PbSeTeO quaternary thin films is dominated by the minimization of the free energy, which consists of the surface energy and strain energy contributions [28]. In the initial stage, the film growth is controlled by the mismatch between the substrate and thin film, leading to the [220] main growth direction due to the lower strain energy compared with the [200] direction [29]. However, the stain energy contribution decreases with the film thickness, leading to the surface energy minimization dominating the grow mechanism, and consequently the [200] main growth direction due to the lower surface energy compared with the [220] direction [30].

The average crystal size, D, the lattice constant, a, and the average micro-strain, ε, of the sputtered thin films were calculated [31, 32], listed in Table 1.

The average crystal size increases with the film thickness, and reaches 47.4 nm when the film thickness is 860 nm, which is similar to the Bohr radius (48 nm) of the PbSe material, indicating that the prominent quantum effect can be obtained in the sputtered PbSeTeO quaternary thin films with the thickness <860 nm [33]. The lattice constant of the sputtered thin films decreases from 6.1612 to 6.1504 Å with the film thickness, which is much larger than the bulk PbSe material (6.124 Å, JCPDS 06-0354) due to the presence of the micro-strain created by the doping tellurium and oxygen atoms in the PbSe crystal lattice [34]. Interestingly enough, the average micro-stain decreases with the film thickness, indicating that growth along the [200] direction can release the strain developed in the sputtered thin films. On the other side, the growth of the crystal size may also release the strain.

3.2 Surface chemistry

Due to the long air exposure, an oxidation layer can be generated on the surface of the PbSe thin films [35]. Moreover, the oxidation layer can act as a passivation layer, which inhibits the surface recombination of the charge carriers, and consequently improves the photoelectric sensitivity of the PbSe thin films [25]. Within this research, XPS measurements were performed before and after the etching treatment to study the chemical states of the elements of the sputtered PbSeTeO quaternary thin films to determine the existence and the content of the oxidation layer, with the results shown in Fig. 3.

The Pb element has two chemical states before and after the etching treatment, as shown in Fig. 3a. The peaks with the binding energy of about 137 eV (Pb4$f_{7/2}$) and 142 eV (Pb4$f_{5/2}$) are attributed to the Pb–Se bonds of PbSe, and the

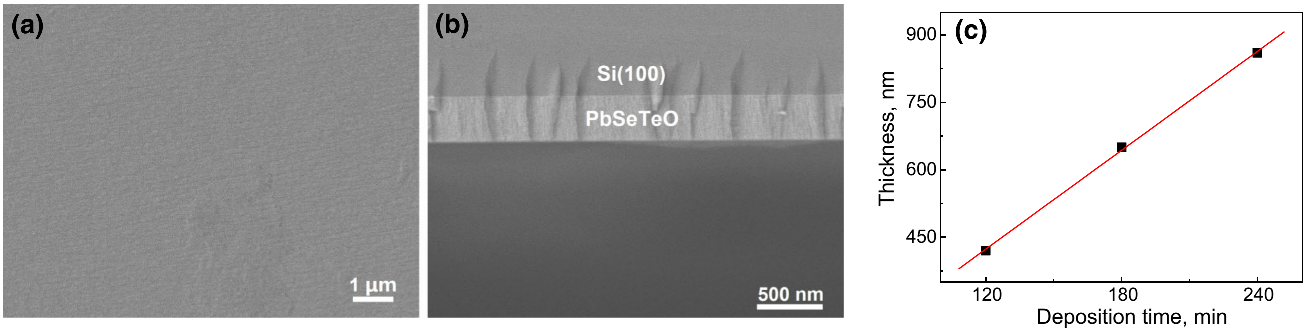

Fig. 1 FE-SEM images of the sputtered PbSeTeO thin films: **a** surface, **b** cross-section, **c** variation of the film thickness with the deposition time

Table 1 Microstructure parameters of the sputtered PbSeTeO quaternary thin films

Sample	Deposition time (min)	δ (nm)	D (nm)	a (Å)	ε ($\times 10^{-3}$)
1	120	420 ± 5	16.6	6.1612	5.99
2	180	650 ± 5	19.7	6.1561	5.24
3	240	860 ± 10	47.4	6.1504	3.02

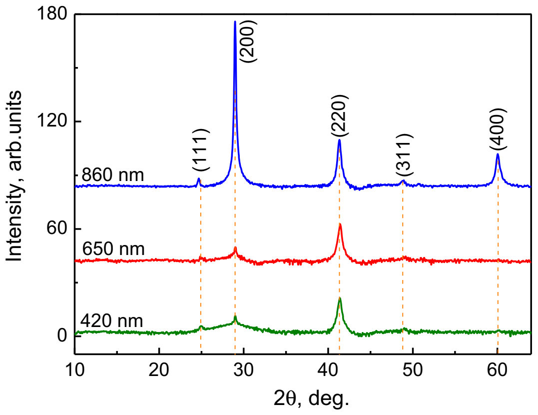

Fig. 2 XRD results of the sputtered PbSeTeO quaternary thin films

peaks at about 138 eV ($Pb4f_{7/2}$) and 143 eV ($Pb4f_{5/2}$) are related to the Pb–O bonds of PbO [36, 37]. Moreover, the PbO content decreases sharply after the etching treatment, indicating the existence of the absorbed oxygen atoms on the surface of the PbSeTeO quaternary thin films. As shown in Fig. 3b, the Se element also has two chemical states before the etching treatment, and the peaks at about 53 eV ($Se3d_{5/2}$) and 54 eV ($Se3d_{3/2}$) are attributed to the Pb–Se bond of PbSe, while the peaks with the binding energy of about 58 eV ($Se3d_{5/2}$) and 59 eV ($Se3d_{3/2}$) are related to the Se–O bond of SeO_2. In addition, the SeO_2 chemical state vanishes after the etching treatment, indicating that oxygen atoms substitute Se atoms and bond with Pb atoms [17]. For the Te element, just one chemical state with the binding energy of 576 eV ($Te3d_{5/2}$) and

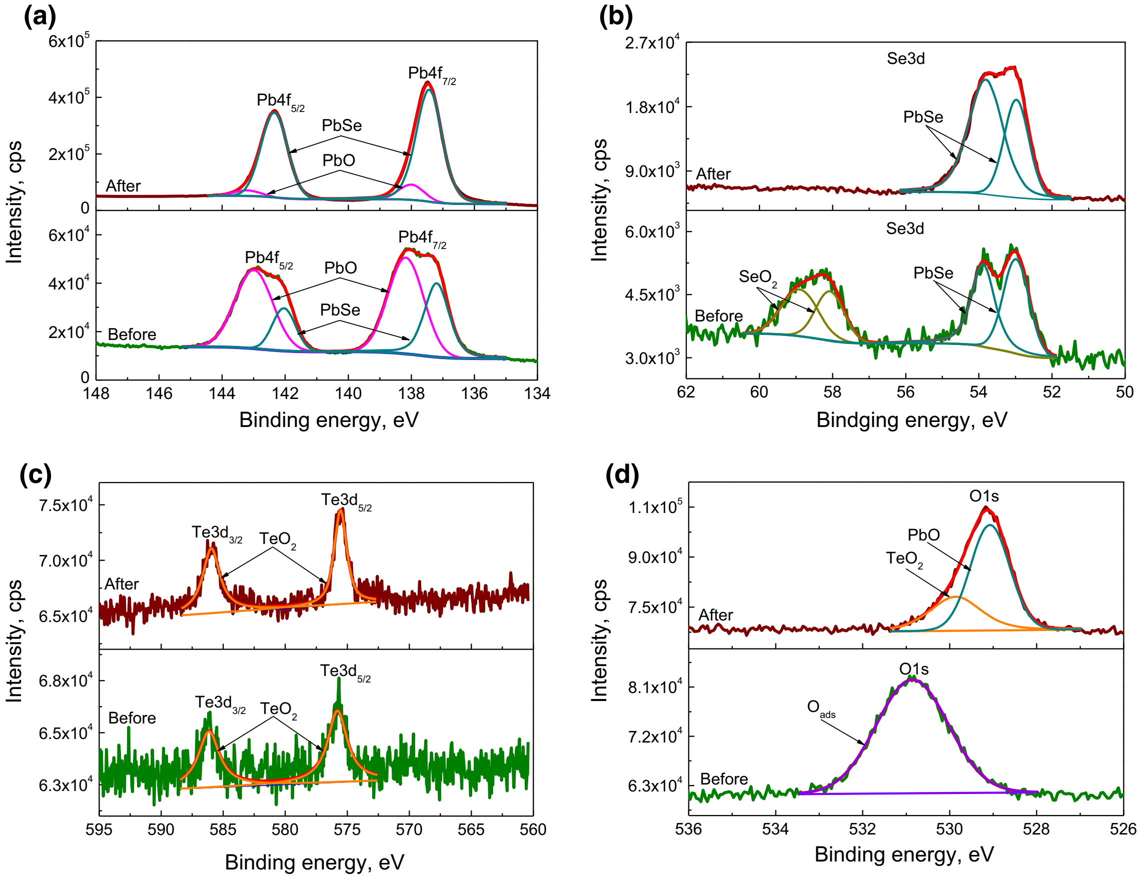

Fig. 3 XPS results of the sputtered PbSeTeO quaternary thin films obtained before and after 120 s etching treatment: **a** Pb4f spectra, **b** Se3d spectra, **c** Te3d spectra, **d** O1s spectra

586 eV ($Te3d_{3/2}$), attributed to the Te–O bonds of TeO_2 was detected, as seen in Fig. 3c [38]. Moreover, the intensity of the peaks increases after the etching treatment, indicating that the Te atoms easily bond with the oxygen atoms during the deposition process. Before the etching treatment, the surface of the PbSeTeO quaternary thin films is covered with absorbed oxygen, which can be removed by Ar^+ etching, as shown in Fig. 3d. Moreover, the oxides after the etching treatment include PbO and SeO_2 two chemical states, in agreement with the above results for the Pb, Se and Te elements.

In summary, an oxidation layer containing PbSe, PbO, SeO_2 and TeO_2 was formed on the sputtered PbSeTeO quaternary thin film surface. Moreover, the content of PbO and SeO_2 decreases sharply after the etching treatment, which is opposite to TeO_2, indicating that the Te atoms are more easily bonded with oxygen atoms during the deposition process. In addition, the content of the oxides contained in the sputtered PbSeTeO quaternary thin films is quite low, leading to the unobservable peaks in the XRD experiments (Sect. 3.1).

3.3 Optical properties

The optical absorption spectra recorded in the infrared regions are related to the electronic transitions, which is useful for understanding the electronic band structure of semiconducting materials [39]. Within this research, the optical properties of the sputtered PbSeTeO quaternary thin films were studied using the infrared absorption spectra recorded from 4000 to 400 cm^{-1} at room temperature, as shown in Fig. 4a. The absorbance of the PbSeTeO quaternary thin films increases with the film thickness. This may be attributed to the more intense scattering absorption of the grain boundaries, consequently leading to larger absorbance of the incident light, confirmed by the XRD results listed in Table 1. Moreover, the absorption edge of the thin films showed a red shift of 2200 cm^{-1} (4.55 μm) to 1400 cm^{-1} (7.14 μm) as the thickness increased, indicating that varying the film thickness is an effective way to change the absorption range of the sputtered PbSeTeO quaternary thin films.

The optical band gap, E_g, is a useful parameter to evaluate the optical and photoelectric properties of the sputtered PbSeTeO quaternary thin films, which can be calculated as follows [39]:

$$(\alpha h\nu)^2 = B(h\nu - E_g) \tag{1}$$

where α is the absorption coefficient, calculated as $\alpha = 1/d \ln(I_0/I)$. Here, I_0 is the incident intensity and I is the intensity after traversing a certain thickness d of the tested thin films. h represents the Planck's constant, ν is the frequency of the incident beam and B is a constant. The E_g values of the sputtered PbSeTeO thin films with the thickness of 420, 650 and 860 nm are 0.29, 0.23 and 0.20 eV, respectively, obtained by extrapolating the linear part of the curve to the energy axis at $(\alpha h\nu)^2 = 0$, as shown in Fig. 4b and Table 2.

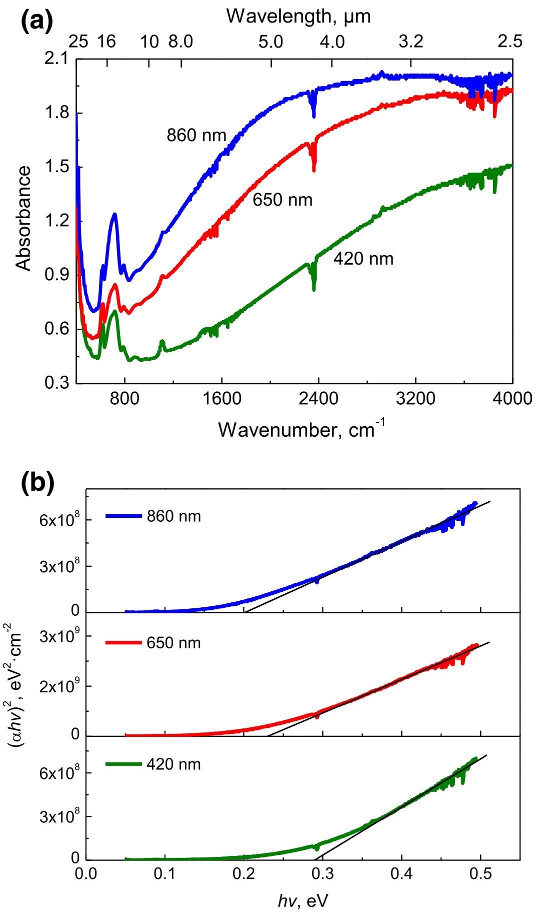

Fig. 4 Optical properties of the sputtered PbSeTeO quaternary thin films: **a** FT-IR absorbance spectra, **b** relationship between the incident beam energy $h\nu$ and $(\alpha h\nu)^2$

Clearly, the E_g values of the sputtered PbSeTeO quaternary thin films decrease with the film thickness, which may be attributed to the lattice constant decrease with the film thickness, leading to weaker bound free electrons. This speculation can be confirmed by the following band structure calculation, based on the GGA with the PBE exchange correlation functional formalism. PbSeTeO supercells with the lattice constant listed in Table 1 were created for the band structure calculation, as illustrated in Fig. 5. The calculated band gap values, E'_g, of the PbSeTeO quaternary crystal decrease from 0.233 to 0.215 eV as the lattice constant decreases from 6.1612 to 6.1504 Å, as shown in Fig. 6 and Table 2. Deviation between the experimental and calculated values is attributed to the underestimation

Table 2 Optical and photoelectric properties of the sputtered PbSeTeO

Sample	E_g (eV)	E'_g (eV)	$\bar{R}_D$ (MΩ)	$\Delta\tilde{R}_t$ (%)	n (1/cm^{3})	μ [cm^2/(V s)]	R_H (cm^3/C)
1	0.29	0.233	2.3	72.4	3.98×10^{13}	1.13	-1.57×10^{5}
2	0.23	0.224	0.925	84.3	8.51×10^{13}	2.18	-0.73×10^{5}
3	0.20	0.215	0.145	92.6	1.34×10^{14}	3.29	-0.46×10^{5}

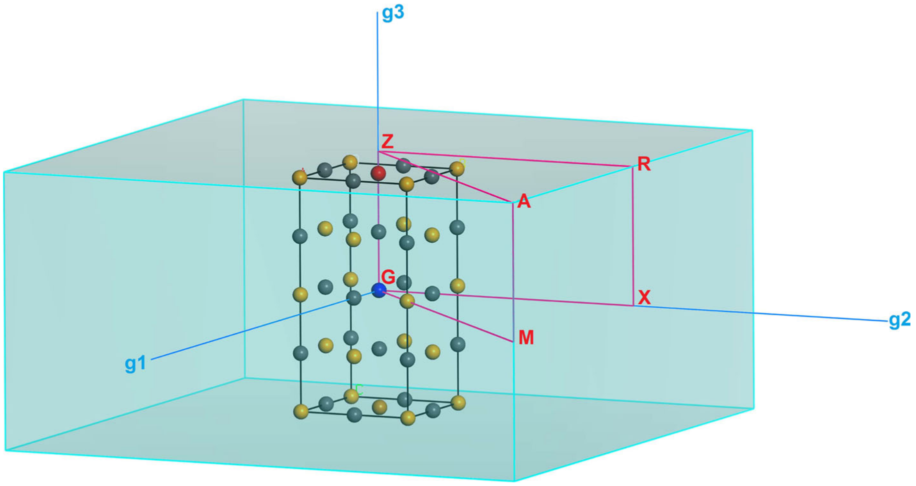

Fig. 5 PbSeTeO supercell. The *dark gray*, *brown*, *red* and *blue spheres* represent Pb, Se, Te and O atoms, respectively. *G* (0, 0, 0), *Z* (0, 0, 0.5), *A* (0.5, 0.5, 0.5), *M* (0.5, 0.5, 0.0), *X* (0.0, 0.5, 0.0) and *R* (0.0, 0.5, 0.5) are the symmetry points of the Brillouin zone (Color figure online)

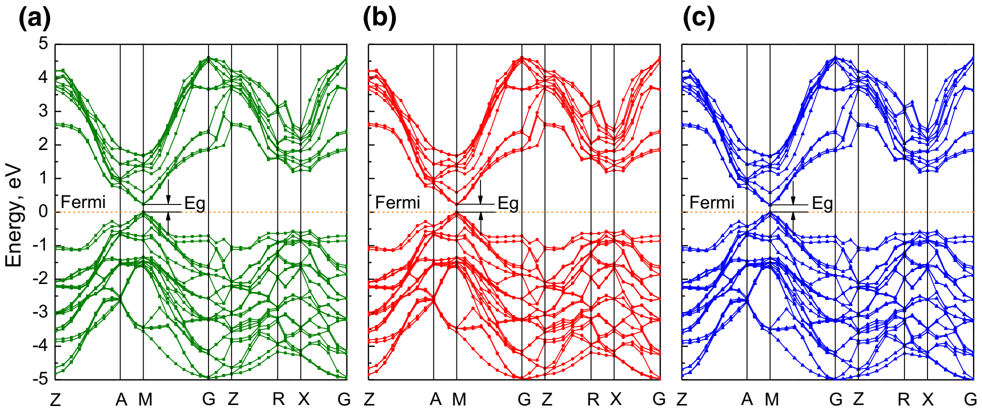

Fig. 6 Band gap structure of the sputtered PbSeTeO quaternary thin films with different thickness: **a** 420 nm, **b** 650 nm, **c** 860 nm

effect of the GGA + PBE functional formalism, however, the varying trend is reliable.

3.4 Photoelectric properties

The difference between the dark and light resistance is a useful parameter to estimate the photoelectric sensitivity of the infrared detector materials [40]. Within this research, the dark and light resistance was obtained using the two-probe method in a dark chamber equipped with a 275 W infrared light source and a digital ohmmeter.

As seen in Fig. 7a, three different regions are collected when the light is turned on and off. The dark resistance remains almost constant before the illumination treatment. After the light turns on, the resistance decreases sharply and reaches saturation after about 40 s of illumination. Finally, the resistance increases slowly after the illumination treatment, indicating that the recombination of the free charge carries is time consuming. Moreover, the dark resistivity of the sputtered PbSeTeO quaternary thin films decreases with the film thickness due to the increase of the free charge carrier concentration and mobility confirmed by the Hall effect measurements, as shown in Fig. 7a inset and Table 2.

Generally, the photoelectric sensitivity of the sputtered PbSeTeO quaternary thin films can be simply represented using $\Delta\tilde{R}_t = \left(\bar{R}_D - R_{L,t}\right)/\bar{R}_D \times 100\,\%$, where $\Delta\tilde{R}_t$ is the resistance change rate between the dark and light resistance at illumination time t, $\bar{R}_D$ is the average value of the dark resistance between 0 and 300 s and $R_{L,t}$ represents the light

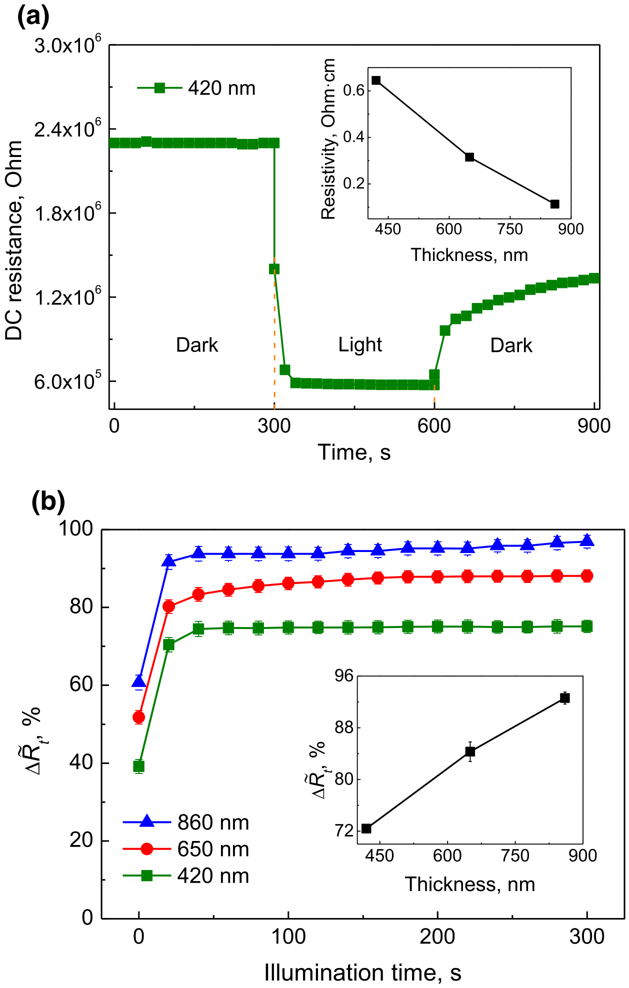

Fig. 7 Photoelectric properties of the sputtered PbSeTeO quaternary thin films: **a** variation of the film resistance in the dark and under certain illumination, **b** resistance change rate under illumination as a function of the illumination time. The *insets* in **a** and **b** show the variation of the dark resistivity and average resistance change rate with the film thickness, respectively

resistance after a certain illumination time, *t*. The $\Delta\tilde{R}_t$ values of the sputtered PbSeTeO quaternary thin films increase with the illumination time, and reach saturation after about 20 s, as shown in Fig. 7b and Table 2. Moreover, the saturation values increase almost linearly with the film thickness, indicating that varying the thickness is an effective way to improve the photoelectric sensitivity of the sputtered PbSeTeO quaternary thin films.

The photoelectric sensitivity of the semiconductor thin films is mainly affected by the concentration and mobility of the photo-generated free charge carriers [41]. However, the mobility of carriers is almost unchanged before and during the illumination, which consequently leads to the photoelectric sensitivity dominated by the concentration contribution [42].

Moreover, the concentration is the dominating factor since the mobility of the free charge carriers is similar for the sputtered thin films. Hence, the PbSeTeO sample with the thickness of 860 nm has higher photo-generated free charge carrier concentration compared with the other two samples, which can be clarified by the calculation results of the DOS, shown in Fig. 8.

The total density of states (TDOS) and the partial density of states (PDOS) provide information about the band

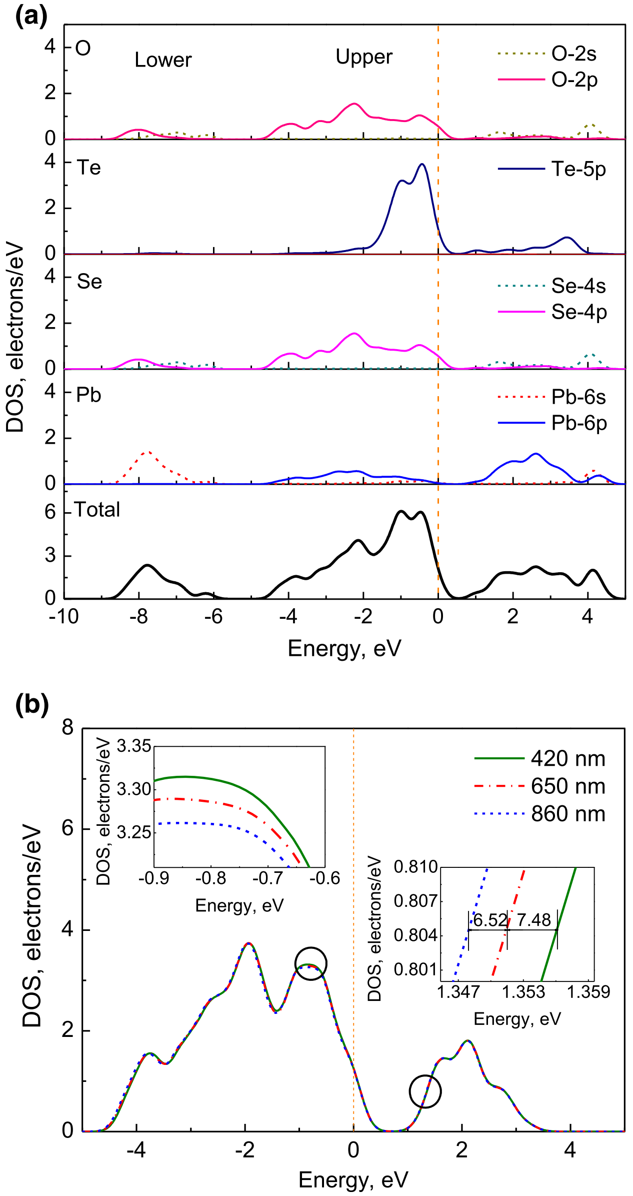

Fig. 8 Density of states of the PbSeTeO quaternary crystal: **a** partial density of states (PDOS) of the PbSeTeO quaternary crystal, **b** density of states of PbSeTeO quaternary crystal with different lattice constant shown in Table 1. The *insets* in **b** show the magnified view of the DOS plots labeled by the *circles*, and the shift in the *right inset* is in meV

structure and the carrier density distribution of the semiconductor materials [14]. As shown in Fig. 8a, the TDOS of the PbSeTeO quaternary thin films is mainly affected by the Pb-6s, Pb-6p, Se-4s, Se-4p, Te-5p, O-2s and O-2p states in the −10 to 5 eV energy range. It is interesting to note that the lower valence band (−9 to −6 eV) is dominated by the Pb-6s states, while the upper valence band (−5 to 0 eV) is mainly occupied by the Se-4p, Te-5p and O-2p states. Moreover, the conduction band is mainly composed of the Pb-6p state and partially occupied by the Se-4s and O-2s states.

The DOS of the PbSeTeO quaternary crystals changes with the lattice constant, as shown in Fig. 8b. The DOS near the top of the valence band decreases with the lattice constant, leading to the decrease of the recombination rate of the photo-generated free charge carriers (electrons and holes). On the other hand, the bottom of the conduction band shifts to lower energy as the lattice constant decreases from 6.1612 to 6.1504 Å, indicating the decrease of the activation energy of the free charge carriers from the valence band to the conduction band, i.e., the increase of the photo-activated charge carrier concentration and consequently the lower photoelectric sensitivity. Besides, the DOS near the bottom of the conduction band increases as the lattice constant decreases from 6.1612 to 6.1504 Å, leading to the increase of the photo-activated charge carrier concentration [43]. The photoelectric sensitivity of the PbSeTeO quaternary thin films increases with the films thickness due to these three reasons, which is in agreement with the resistance change rate results.

4 Conclusions

Three sputtered PbSeTeO quaternary thin films with different thickness were successfully grown on the Si(100) substrates by magnetron sputtering. The main growth direction of the sputtered thin films changes from [220] to [200] as the thickness exceeds 650 nm due to the transition between the surface and strain energy contributions to the total free energy. An oxidation layer, which contains PbSe, PbO, SeO_2 and TeO_2, is formed on the film surface due to the exposure to oxygen. However, the content of the oxides contained in the thin films is low.

The absorption edge of the thin films shows a prominent red shift of 2200 cm^{-1} (4.55 μm) to 1400 cm^{-1} (7.14 μm) as the thickness increases from 420 to 860 nm, corresponding to the optical band gap of 0.29 and 0.2 eV. The photoelectric sensitivity of the sputtered PbSeTeO quaternary thin films increases almost linearly with the film thickness due to the decrease of DOS at the top of the valence band, the narrowing of the optical band and the increase of DOS at the bottom of the conduction band with the film thickness.

Acknowledgments This work was supported by the National Nature Science Foundation of China (51271022), the Fok Ying Tung Education Foundation (132001) and the Fundamental Research Funds for the Central Universities (FRF-TP-14-008A2). Alex Volinsky acknowledges support from the National Science Foundation under the IRES 1358088 Grant.

References

1. J.M. Martin, J.L. Hernández, L. Adell, A. Rodriguez, F. López, Arrays of thermally evaporated PbSe infrared photodetectors deposited on Si substrates operating at room temperature. Semicond. Sci. Technol. **11**, 1740–1744 (1996)
2. H. Preier, Recent advances in lead-chalcognide diode lasers. Appl. Phys. **20**, 189–206 (1979)
3. J.P. Heremans, V. Jovovic, E.S. Toberer, A. Saramat, K. Kurosaki, A. Charoenphakdee, S. Yamanaka, G.J. Snyder, Enhancement of thermoelectric efficiency in PbTe by distortion of the electronic density of states. Science **321**, 554–557 (2008)
4. J.J. Choi, Y.F. Lim, M.B. Santiago-Berrios, M. Oh, B.R. Hyun, L.F. Sun, A.C. Bartnik, A. Goedhart, G.G. Malliaras, H.D. Abruña, F.W. Wise, T. Hanrath, PbSe nanocrystal excitonic solar cells. Nano Lett. **9**, 3749–3755 (2009)
5. E.A. Albanesi, E.L.P.Y. Blanca, A.G. Petukhov, Calculated optical spectra of IV–VI semiconductors PbS, PbSe and PbTe. Comput. Mater. Sci. **32**, 85–95 (2005)
6. Y.I. Ravich, B.A. Efimova, I.A. Smirnov, *Semiconductoring Lead Chalcogenides* (Springer Science + Business Media, New York, 1970)
7. K.C. Preetha, T.L. Remadevi, Band gap engineering in PbSe thin films from near-infrared to visible region by photochemical deposition method. J. Mater. Sci. Mater. Electron. **25**, 1783–1791 (2014)
8. R. Basu, S. Bhattacharya, R.R. Bhatt, A. Singh, D.K. Aswal, S.K. Gupta, Improved thermoelectric properties of Se-doped n-type $PbTe_{1-x}Se_x$ $(0 \leq x \leq 1)$. J. Electron. Mater. **42**, 2292–2296 (2013)
9. A.J. Strauss, T.C. Harman, Pseudobinary phase diagram and existence regions for $PbS_{1-x}Se_x$. J. Electron. Mater. **2**, 71–85 (1973)
10. H. Zogg, A. Fach, J. John, J. Masek, P. Muller, C. Paglino, W. Buttler, $Pb_{1-x}Sn_xSe$-on Si LWIR sensor arrays and thermal imaging with JFET/CMOS read-out. J. Electron. Mater. **25**, 1366–1370 (1996)
11. M.I. Baleva, M.H. Maksimov, S.M. Metev, M.S. Sendova, Laser-assisted sputtering of $Pb_{1-x}Cd_xSe$ films. J. Mater. Sci. Lett. **5**, 533–536 (1986)
12. W.Z. Shen, Observation of exciton localization in PbSrSe thin films grown by molecular beam epitaxy. Appl. Phys. A **80**, 389–394 (2005)
13. S. Kumar, M. Hussain, T.P. Sharma, M. Husain, Characterization of $PbSe_{1-x}Te_x$ thin films. J. Phys. Chem. Solids **64**, 367–376 (2003)
14. G. Naeemullah, R. Murtaza, N. Khenata, S. Hassan, M.N. Naeem, S.B. Khalid, Omran. Structural and optoelectronic properties of PbS_xSe_{1-x}, PbS_xTe_{1-x} and $PbSe_xTe_{1-x}$ via first-principles calculations. Comput. Mater. Sci. **83**, 496–503 (2014)
15. F. Zhao, S. Mukherjee, J. Ma, D. Li, S.L. Elizondo, Z. Shi, Influence of oxygen passivation on optical properties of PbSe thin films. Appl. Phys. Lett. **92**, 1–3 (2008)

16. C. Gautier, M.C. Muller, M. Averous, Study of PbSe layer oxidation and oxide dissolution. Appl. Surf. Sci. **141**, 157–163 (1999)
17. H. Jung, R. Kuljic, M.A. Stroscio, M. Dutta, Confinement in PbSe wires grown by rf magnetron sputtering. Appl. Phys. Lett. **96**, 153106 (2010)
18. I. Grozdanov, M. Najdoski, S.K. Dey, A simple solution growth technique for PbSe thin films. Mater. Lett. **38**, 28–32 (1999)
19. N. Mukherjee, A. Mondal, Comparative study on the properties of galvanically deposited nano- and microcrystalline thin films of PbSe. J. Electron. Mater. **39**, 1177–1185 (2010)
20. S. Gad, M.A. Rafea, Y. Badr, Optical and photoconductive properties of $Pb_{0.9}Sn_{0.1}Se$ nano-structured thin films deposited by thermal vacuum evaporation and pulsed laser deposition. J. Alloys Compd. **515**, 101–107 (2012)
21. D. Li, J. Ma, S. Mukherjee, G. Bi, F. Zhao, S.L. Elizondo, Z. Shi, A new *in-situ* surface treatment during MBE-grown PbSe on CaF_2/Si(111) heterostructure. J. Cryst. Growth **311**, 3395–3398 (2009)
22. P.J. Kelly, R.D. Arnell, Magnetron sputtering: a review of recent developments and applications. Vacuum **56**, 159–172 (2000)
23. A. Jdanov, J. Pelleg, Z. Dashevsky, R. Shneck, Growth and characterization of PbTe films by magnetron sputtering. Mater. Sci. Eng. B **106**, 89–94 (2004)
24. M. Lach-hab, D.A. Papaconstantopoulos, M.J. Mehl, Electronic structure calculations of lead chalcogenides PbS, PbSe, PbTe. J. Phys. Chem. Solids **63**, 833–841 (2002)
25. W.R. Feng, H. Zhou, F. Chen, Impact of thickness on crystal structure and optical properties for thermally evaporated PbSe thin films. Vacuum **114**, 82–85 (2015)
26. M.S. Raven, ESCA interface study of ion-plated and thermally evaporated selenium films. J. Phys. D Appl. Phys. **11**, 631–642 (1978)
27. V. Consonni, G. Rey, H. Roussel, D. Bellet, Thickness effects on the texture development of fluorine-doped SnO_2 thin films: the role of surface and strain energy. J. Appl. Phys. **111**, 033523–033523-7 (2012)
28. X.J. Wang, Y.B. Hou, Y. Chang, C.R. Becker, R.F. Klie, R. Kodama, F. Aqariden, S. Sivananthan, Growth of PbSe on ZnTe/GaAs(211)B by molecular beam epitaxy. J. Cryst. Growth **312**, 910–913 (2010)
29. J.E. Petersen, L.M. Scolfaro, T.H. Myers, Elastic and mechanical properties of intrinsic and doped PbSe and PbTe studied by first-principles. Mater. Chem. Phys. **146**, 472–477 (2014)
30. W.R. Feng, X.Y. Wang, F. Chen, W. Liu, H. Zhou, S. Wang, H.R. Li, Influence of substrate temperature on structural, morphological and electrical properties of PbSe film deposited by radio frequency sputtering. Thin Solid Films **578**, 25–30 (2015)
31. S. Thanikaikarasan, T. Mahalingam, V. Dhanasekaran, A. Kathalingam, J.K. Rhee, Growth and characterization of lead selenide thin films. J. Mater. Sci. Mater. Electron. **23**, 1562–1568 (2012)
32. M.M. Parvathi, V. Arivazhagan, S. Rajesh, Structural and optical properties of ZnSe thin films stacked with PbSe submonolayers. Appl. Phys. A **116**, 1773–1778 (2014)
33. W.L. Ma, J.M. Luther, H.M. Zheng, Y. Wu, A.P. Alivisatos, Photovoltaic devices employing ternary PbS_xSe_{1-x} nanocrystals. Nano Lett. **9**, 1699–1703 (2009)
34. A. Begum, A. Hussain, A. Rahman, Effect of deposition temperature on the structural and optical properties of chemically prepared nanocrystalline lead selenide thin films. Beilstein J. Nanotechnol. **3**, 438–443 (2012)
35. A.D.R. Pillai, K. Zhang, K. Bollenbach, D. Nminibapiel, W. Cao, H. Baumgart, V.S.K. Chakravadhanula, C. Kübel, V. Kochergin, ALD growth of PbTe and PbSe superlattices for thermoelectric applications. ECS Trans. **10**, 131–139 (2013)
36. S.X. Lin, X. Zhang, X.Z. Shi, J.P. Wei, D.B. Lu, Y.Z. Zhang, H.H. Kou, C.M. Wang, Nanoscale semiconductor $Pb_{1-x}Sn_xSe$ ($x = 0.2$) thin films synthesized by electrochemical atomic layer deposition. Appl. Surf. Sci. **257**, 5803–5807 (2011)
37. J.M. Luther, M. Law, Q. Song, C.L. Perkins, M.C. Beard, A.J. Nozik, Structural, optical, and electrical properties of self-assembled films of PbSe nanocrystals treated with 1, 2-ethanedithiol. ACS Nano **2**, 217–280 (2008)
38. O.A. Balitskii, W. Jaegermann, XPS study of InTe and GaTe single crystals oxidation. Mater. Chem. Phys. **97**, 98–101 (2006)
39. A.A. Al-Ghamdi, S. Al-Heniti, S.A. Khan, Structural, optical and electrical characterization of Ag doped lead chalcogenide (PbSe) thin films. J. Lumin. **135**, 295–300 (2013)
40. P.K. Nair, E.B. Salgado, J. Capistrán, M.L. Ramón, M.T.S. Nair, R.A. Zingaro, PbSe thin films in all-chemically deposited solar cells. J. Electronchem. Soc. **10**, D528–D537 (2010)
41. S.V. Streltsov, A.Y. Manakov, A.P. Vokhmyanin, S.V. Ovsyannikov, V.V. Shchennikov, Crystal lattice and band structure of the intermediate high-pressure phase of PbSe. J. Phys. Condens. Matter **21**, 385501 (2009)
42. S.H. Wei, Al Zunger, Electronic and structural anomalies in lead chalcogenides. Phys. Rev. B **1**, 13605 (1997)
43. E.A. El-Sayad, B.S. Farag, A.T. Amin, Electrical properties of crystalline $Pb_xSn_{1-x}Te_{0.5}Se_{0.5}$ thin films. Vacuum **84**, 807–811 (2010)